Normal-Force Characteristics of Sharp-Edged Delta Wings at Supersonic Speeds

Erik S. Larson*
FFA, The Aeronautical Research Institute of Sweden, Bromma, Sweden

An engineering method for estimating the normal-force characteristics of sharp-edged delta wings at supersonic speeds is under development, and the first result is presented. The method utilizes experimental results from several sources and basic flow characteristics such as the vacuum limit, the pressure loss factor, and the face drag of disks. Experimental lift-curve slope data show that the wing thickness-to-chord ratio cannot be ignored, and therefore the present result is prepared for wings with a fixed profile apex half-angle in the flow direction. The analytic expressions for various partial contributions to the normal force of the delta wing are relatively simple and represent experimental data quite satisfactorily. To improve the engineering method, an accurate knowledge of the partitioning of the attached-flow lift-curve slope between the upper and lower surfaces of the delta wing is needed from experiments and/or higher-order flow theories.

Nomenclatures

A = aspect ratio $= b^2/S = 4s^2/S = 4\tan\epsilon$
a = normal-force-curve slope ratio
b = wing span
C_D = drag coefficient
C_L = lift coefficient
C_N = normal-force coefficient
C_N^ℓ = wing lower side normal-force coefficient
C_N^u = wing upper side normal-force coefficient
$C_{N,v}$ = vortex-induced normal-force coefficient
e = transonic thickness parameter
f = pressure loss factor
K = shape factor
K_v = vortex-induced normal-force-curve slope
M = Mach number
M_n = Mach number normal to wing leading edge $= M\cos\Lambda_{LE}(1+\tan\alpha/\cos\Lambda_{LE})^{1/2}$
m = $\beta\tan\epsilon$
s = wing half-span
S = wing surface
α = angle of attack
α_n = angle of attack normal to wing leading edge $= \tan^{-1}(\tan\alpha/\sin\epsilon)$
$\tilde{\alpha}_n$ = $\alpha_n\beta\tan\epsilon$
β = $\sqrt{M^2-1}$
γ = ratio of specific heats
δ_{LE} = deflection angle of wing leading edge
ϵ = wing apex half-angle
Λ_{LE} = leading-edge sweep angle
μ = Mach angle
θ = profile apex half-angle

Subscripts

$,DF$ = front surface drag
α = slope vs angle of attack
ℓ = lower surface
$,p;p$ = attached (potential) flow
nf = normal to disk front surface
u = upper surface
$,v$ = vortex-induced
$,s$ = separation

Received Nov. 7, 1986; revision received Dec. 18, 1986; presented as Paper 87-0214 at the AIAA 25th Aerospace Sciences Meeting, Reno, NV, Jan. 12-15, 1987.

*Senior Research Engineer, Aerodynamics Department. Member AIAA.

Introduction

A RENEWAL of the interest in the flow mechanics and force characteristics of delta wings at supersonic speeds has recently become apparent, i.e., for flows with Mach numbers well above unity but still low enough to leave the leading edge subsonic. In this speed region, the possibility exists of taking advantage of the leading-edge suction force in reducing the induced drag. This circumstance in combination with the improvements of the thrust-to-weight ratio of the turbojet engine has opened up new challenges for the designer. Thus, in the middle of the next decade, several fighter aircraft will probably appear with the capacity to perform very high load-factor maneuvers at supersonic speeds without loss of speed by using only engine dry thrust. For such a development, improved insight into delta wing characteristics at supersonic speeds is of crucial importance.

The evolution of knowledge about supersonic flowfields began about 45 years ago. In the early stages of building up knowledge about the aerodynamic characteristics of delta wings at supersonic speeds, linearized theory played an important role. Stewart[1] presented a solution for the lift-curve slope in 1946. In 1953, Adams and Sears[2] obtained a similar result from slender-body theory for Mach numbers up to the sonic leading edge. Of no less importance than theory for gaining insight into the flow phenomena around delta wings at supersonic speeds was the wind tunnel. Thus the comprehensive experimental investigations of delta wings at supersonic speeds conducted by Lampert[3,4] and Love[5] gave the first broad view of real-flow data and their dependence upon the Mach number and aspect ratio. For instance, a large discrepancy between theory and experiment in the lift-curve slope in a wide interval around sonic leading-edge flow conditions emerged. This discrepancy evidently could be related to the thickness-to-chord ratio of the wing. The experimental results[3-5] since then have been a most valuable data resource for design studies and were empirically respresented by the analytic expressions in Ref. 6 primarily for use in missile design studies.

As for vortex flows around delta wings, the early theoretical solutions for the low-speed flow problem by Legendre[7] (1952) and Edwards[8] (1954) gave the impetus to a great number of theoretical studies. Unfortunately these were not followed by corresponding solutions for supersonic speeds. The high com-

plexity of vortex flows and the difficulty of obtaining an accuracy suitable for practical use has given priority to numerical solutions. The rapid evolution of computational approaches in the field of vortex flows cannot be evaluated here. Recent results obtained with various types of panel method applications to the delta wing in supersonic flow have been discussed by Wood and Miller.[9,10] The results are promising but refinements are still needed. A recent solution of the Euler equations for a 70-deg delta wing at $M=1.5$ obtained by Murman, Rizzi, and Powell[11] seems to have the capacity to reproduce most of the experimentally observed flowfield characteristics. Numerous integrations of pressure distributions are needed, however, for comparisons with experiments before comprehensive accuracy tests can be done. Cumbersome numerical solutions, necessary for the scientific clarification of the detailed real-flow characteristics, can hardly be expected to become flexible tools for early project design considerations in the near future.

A recent contribution to the engineering understanding of the specific supersonic speed characteristics of delta wings was presented by Wood and Miller.[9,10] It was obtained through a careful inspection of theoretical and experimental results. By efficient transformations of the angle of attack, they succeeded in exposing different dominating influences of typical parameters on the partial lift contributions from the upper and lower surface of the delta wing.

In the present paper, the results of Lampert,[3,4] Love,[5] and Wood and Miller[9,10] are used in the construction of an engineering method for the rapid estimation of the normal-force characteristics of delta wings at supersonic speeds. Basic real-flow characteristics, such as the vacuum limit, the pressure loss factor, and the face drag of disks, are used to build up the nonlinear contributions in the analytic representations of the partial normal forces. It will be seen that an accurate partitioning of the attached-flow lift-curve slope between the upper and lower surfaces of the wing is needed to improve the engineering method. At present, such a partitioning has to rely upon reasonable assumptions only. Experiments and solutions of a higher order and preferably viscous flow theories must be used, however, to obtain the final answer in this case.

Normal Force Characteristics

Lift-Curve Slope of Delta Wings at Supersonic Speeds

Engineering methods for rapid estimations of the basic aerodynamic characteristics of typical vehicle components are practical tools, especially in the early project design phase when flexibility is of value. Compact analytic expressions also save space in aerodynamics prediction codes and thus shorten the computation time.

In applied aerodynamics, a reasonable estimation of the lift-curve slope for the wing is needed in most situations. As regards the lift-curve slope of delta wings at supersonic speeds, early theoretical solutions were obtained from linearized theory[1] and slender-body flow theory.[2] The solutions show an increasing discrepancy when the reduced aspect ratio parameter $m=\beta\tan\epsilon$ increases to unity. Thereafter, the former solution becomes equal to Ackeret's result and the latter solution stops at $m=1$. The difference between the solutions is in itself of theoretical interest, but it is also disturbing from a practical point of view.

The wind tunnel test[3-5] with sharp-edged delta wing models showed that the general trend of the experimental lift-curve slope over the parameter $\beta\tan\epsilon$ was more in accord with the slender-body theory result[2] than with that obtained from the linearized theory.[1] It also became evident that the thickness of the wing could not be discarded if a good accuracy of the lift-curve slope was to be acquired.

The classical solutions[1,2] for the lift-curve slope are shown in Fig. 1, where an empirically constructed curve from Ref. 6 is also plotted. The latter curve had been found to make an empirical representation of the experimental results[3-5] easier than did a curve representing the classical solutions. The curve is expressed by the chain ratios

$$\frac{\beta}{4}C_{L_\alpha}=\cfrac{(\pi/2)m}{1+\cfrac{(2/3)(\pi/2)\ m^2}{1+\cfrac{(2/3)(\pi/2)\ m^2}{1+m}}}=C(m) \tag{1}$$

where $m=\beta\tan\epsilon$.

With the definition of the aspect ratio $A=4\tan\epsilon$, Eq. (1) has the limit values

$$\lim_{A\to 0}\frac{dC_{L_\alpha}}{dA}=\frac{\pi}{2}\quad\text{and}\quad\lim_{A\to\infty}\frac{dC_{L_\alpha}}{dA}=\frac{2\pi}{\beta} \tag{2}$$

The latter limit value is preferred in this case in lieu of Ackeret's result.

A good coorelation with the experimental results[3-5] was obtained by multiplying the left-hand side of Eq. (1) by the function

$$f\left\{\frac{\epsilon+e}{\mu}\right\}\frac{\beta}{4}C_{L_\alpha}=C(m) \tag{3}$$

where μ is the Mach angle, e is the transonic thickness parameter

$$e=[(\gamma+1)\theta M^2]^{2/3}/\beta^2,\qquad[\epsilon<35\text{ deg}] \tag{4a}$$

and θ is the profile apex half-angle measured along the chord of the delta wing. Equation (4a) is used for slender and not-so-slender delta wings. For less swept delta wings, the simplification

$$e=[(\gamma+1)\theta]^{2/3},\qquad[\epsilon>35\text{ deg}] \tag{4b}$$

gives a better correlation with experiments for $\beta\tan\epsilon<1.25$ than does Eq. (4a). The function f was given the form

$$\log f=[3\theta-(\theta\beta\tan\epsilon)^2]\log\left(\frac{\epsilon+e}{\mu}\right) \tag{5}$$

With a deeper understanding of the physics of the flow, the term in square brackets in Eq. (5) could probably be simplified. With a desk calculator the exponent does little

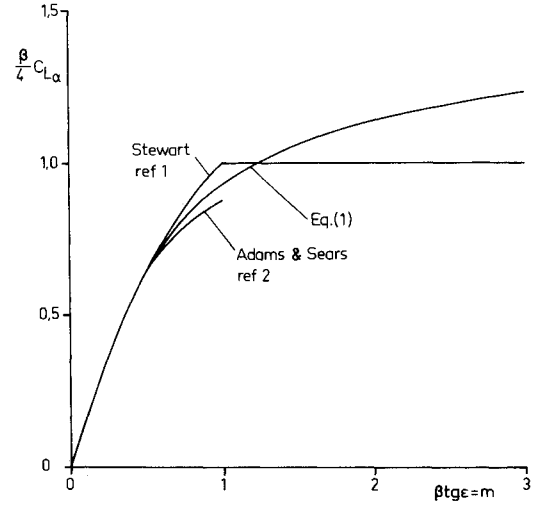

Fig. 1 Lift-curve slope of delta wings vs aspect ratio parameter from linearized theory[1] and slender-body-theory[2] and assumed curved for empirical representation, Eq. (1).

harm, however, and the compactness of the expression is a good excuse for its present analytic form.

The lift-curve slope, represented by Eqs. (3-5), is plotted in Fig. 2 for comparison with Lampert's experimental results[3,4] for three sharped-edged delta wings with aspect ratios $A = 0.858$, 1.433, and 3.616 and $\theta = 6$ deg for all three of them. The Mach number ranges from $M = 1.45$ to 4.55. A similar comparison is made in Fig. 3, where the test results from Love's[5] investigation are shown for a thin ($\theta = 2.86$ deg) delta wing and some thick ($\theta = 12.52$ deg) ones of different aspect ratios.

Normal Force on the Lower Surface of the Delta Wing

The lower surface contribution to the normal force on flat, sharp leading-edge delta wings presented by Wood and Miller[9,10] and the original data received by courtesy of R. M. Wood in the interval of $0.5 < \beta \tan\epsilon < 1$ are represented analytically in Ref. 14. The expressions are

$$C_N^{\ell} = (C_{N_\alpha}^{\ell})_p \sin\alpha \quad \cos\alpha + C_{D_{nf}} \quad \sin^2\alpha < C_{D_{nf}} \tag{6}$$

where

$$(C_{N_\alpha}^{\ell})_p = a_\ell C_{N_\alpha} \tag{7}$$

and

$$a_\ell = 0.41[1 + (\beta \tan\epsilon - 0.7)\sqrt{\sin\epsilon}] \tag{8}$$

The formal resemblance between Eq. (6) and the traditional method of estimating the normal force on slender bodies at high angles of attack should be observed. The nonlinear term in Eq. (6) is represented by the face drag coefficient of disks at 90 deg to the freestream compiled from experiments by Hoerner[12] and represented analytically in Refs. 12 and 13.

The important observation made in Refs. 9 and 10 that C_N^{ℓ} is almost independent of the Mach number was satisfied by the empirical assumption about a_ℓ shown in Eq. (8). Equations (6-8) are applicable in the interval of $0.5 < \beta \tan\epsilon < 1$. In Fig. 4, C_N^{ℓ} as a function of the incidence normal to the leading edge α_n for several sweep angles Λ_{LE} is compared with the result of R. M. Wood.

Normal Force on the Upper Surface of the Delta Wing

It has been found that the normal-force contribution from the upper surface of the delta wing, as presented by Wood and Miller[9,10] over the transformed angle of attack $\bar{\alpha}_n$, can be represented quite satisfactorily by the expression

$$C_N^u = \bar{\gamma}\left[1 + \left(\frac{2}{\gamma M^2} - 0.56\right)\cos^2 2\bar{\alpha}_n\right] \sin 2\bar{\alpha}_n \tag{9}$$

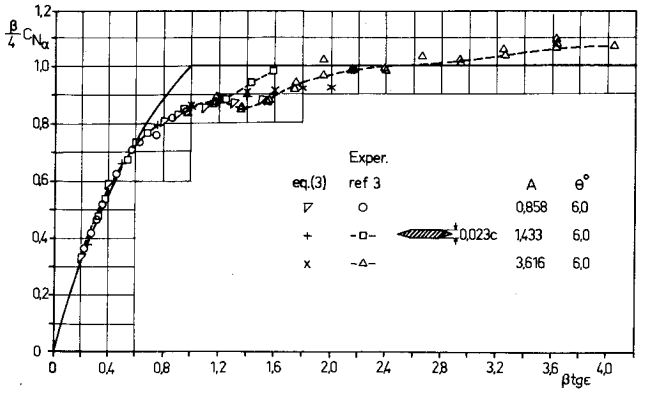

Fig. 2 Empirical representation of $(\beta/4)C_{N_\alpha}(A,\theta)$ vs $\beta \tan\epsilon$ from experiments, Ref. 3, with sharp-edged delta wings for $M = 1.45$–4.55.

where

$$\bar{\gamma} = (2/\gamma M^2)[1 - (1 - f)\sin^2 2\bar{\alpha}_n] \tag{10}$$

and

$$\bar{\alpha}_n = \alpha_n \beta \tan\epsilon \tag{11}$$

with

$$\tan\alpha_n = \tan\alpha / \sin\epsilon \tag{12}$$

and f being what herein might be called "the vacuum limit efficiency factor," also quantified in Ref. 10. This factor is strongly dependent upon the Mach number and varies from 1 to 0.75 from low supersonic speeds to $M = 3.5$

Subtracting the attached-flow contribution (the potential-flow part) from Eq. (9) gives the vortex flow-induced part of

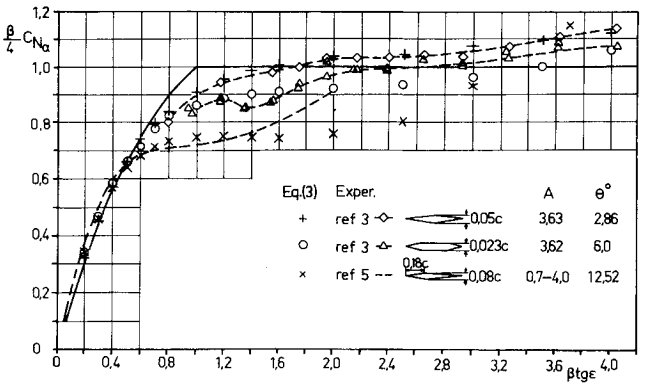

Fig. 3 Empirical representation of $(\beta/4)C_{N_\alpha}(A,\theta)$ vs $\beta \tan\epsilon$ from experiments, Ref. 3 ($M = 1.45$–4.55) and Ref. 5 ($M = 1.6$–2.4), with sharp-edged delta wings.

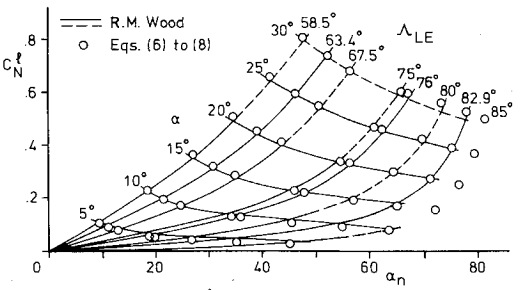

Fig. 4 Representation of $C_N^{\ell}(\Lambda_{LE},M)$ vs α_n for flat delta wings, according to Refs. 9, 10, and 14.

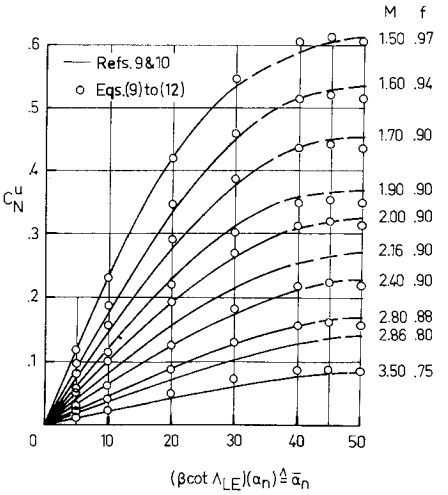

Fig. 5 Representation of $C_N^u(M,\Lambda_{LE})$ vs $\bar{\alpha}_N$ for flat delta wings, according to Refs. 9 and 10.

the normal force on the upper surface of the delta wing:

$$C_{N,v} = C^u_N - C^u_{N,p} \tag{13}$$

where

$$C^u_{N,p} = (C^u_{N_{\bar\alpha_n}})_p \sin\bar\alpha_n \cos\bar\alpha_n \tag{14}$$

and

$$(C^u_{N_{\bar\alpha_n}})_p = (\cos\epsilon/\beta) a_u (C_{N_\alpha})_p \tag{15}$$

$$a_u = 1 - a_\ell \tag{16}$$

The last factor on the right hand side of Eq. (15) is the normal-force-curve slope for the delta wing, according to Eq. (3). C_{N_α} is herein used synonymously with C_{L_α}, because $C_{N_\alpha} \simeq C_{L_\alpha}$. The factor $\cos\epsilon/\beta$ comes from the transformation of α into $\bar\alpha_n$, and a_u is the ratio of the upper-surface lift-curve slope to the total lift-curve slope of the delta wing for an attached flow. The ratios a_u and a_ℓ in Eq. (16) are not adequately known at present and can thus be obtained by assumption only.

Inserting Eqs. (9) and (14) into Eq. (13), dividing with $\sin 2\bar\alpha_n$, and letting $\bar\alpha_n$ approach zero gives

$$\frac{\partial C_{N,v}}{\partial(\sin 2\bar\alpha_n)} = K_v = \frac{2}{\gamma M^2}\left[1 + \left(\frac{2}{\gamma M^2} - 0.56\right)\right] - \frac{1}{2}(C^u_{N_{\bar\alpha_n}})_p \tag{17}$$

K_v thus receives a finite value when $\bar\alpha_n$ approaches zero.

The Normal Force of the Delta Wing

Adding the upper and lower surface contributions gives the normal-force coefficient of the flat, sharp-edged delta wing in the interval of $0.5 < \beta\tan\epsilon < 1$, investigated in Refs. 9 and 10. Different forms of the coefficient can be expressed. Perhaps the most straightforward one involves explicit attached-(potential) and vortex-flow contributions. Thus

$$C_N = C^u_N + C^\ell_N = C_{N,p} + C_{N,v} + C_{N,Df}$$
$$= C_{N_{\alpha,p}} \sin\alpha\cos\alpha + C_{N,v} + C_{D_{nf}} \sin^2\alpha \tag{18}$$

The first and third coefficients are defined in the α-plane and are obtained from Eq. (3) and Eq. (6) with their auxiliary equations respectively. $C_{N,v}$, on the other hand, is defined in the $\bar\alpha_n$-plane, according to Eq. (17). Because of the several trigonometric terms involved, it seems practical to evaluate the $C_{N,v}$ term as it stands and transform α into $\bar\alpha_n$ separately. From the slope of the vortex normal-force curve, Eq. (17), and Eq. (15), it is seen that the ratio a_u is the only unknown in the expression for $C_{N,v}$. It can be noticed that linearized theory gives $a_u = a_\ell = 0.5$, and that this is not in accord with real-flow characteristics at supersonic speeds. Formally, a_u could be obtained from Eq. (16) if a_ℓ were accurately known. This is not the case at present, however, because the empirical expression for a_ℓ in Eq. (8) most probably contains a correction for effects that in reality should not be referred to a_ℓ. Therefore, the ratio a_u, when used herein, has been obtained by either fitting to the experimental results or by assumption only. The ratio thus obtained will be depicted $\bar a_u$ because it does not represent the true a_u for $\alpha \to 0$, but might very well be a function of the incidence of the wing.

Because of the present uncertainty as to a_u, an expression for the total normal force is instead compiled from the better-known quantities, Eqs. (6) and (9), as

$$C_N = C^u_N + C^\ell_N = C^u_N + C^\ell_{N,p} + C_{N,Df} \tag{19}$$

In order to obtain a simple sensitivity test, the face drag term in Eq. (6) is modified by introducing a zero angle correction, α_o. Equation (19) then takes the form

$$C_N = C^u_N + C^\ell_{N,p} + C_{D_{nf}} \sin|\alpha - \alpha_0| \sin(\alpha - \alpha_0), \quad |\alpha| > |\alpha_0| \tag{20}$$

Results

The analytic representation of the upper-surface normal force $C^u_N(\bar\alpha_n; M)$ by Eqs. (9–12) is compared with the set of curves obtained by Wood and Miller[9,10] in Fig. 5. The loss factors f inserted into the figure are taken from Ref. 10, except for $M = 1.6$, where $f = 0.94$ has been used instead of $f = 0.9$, which seems to represent too low a value.

The result of using Eqs. (13–15), representing the vortex-induced normal-force coefficient $C_{N,v}$, in a curve fitting procedure to find $\bar a_u$ for a $\Lambda_{LE} = 75$-deg wing is shown in Fig. 6, which is a replot of Fig. 13 from Ref. 9. Inserted into Fig. 6 are $C_{N,v}$ curves for a varying $\bar a_u$ for comparison with the experimental data for 1) the variation of M at $\alpha = 16$ deg, and 2) the variation of α at $M = 1.7$. A similar sensitivity test of $C_{N,v}$ to $\bar a_u$ for a $\Lambda_{LE} = 58$-deg wing is shown in Fig. 7 vs low supersonic Mach numbers at $\alpha = 12$ deg and vs α at $M = 1.5$.

A subdivision of the total normal-force of the $\Lambda_{LE} = 75$- and 58-deg wings at $M = 1.7$ and 1.5, respectively, into the four partial contributions discussed herein is shown in Fig. 8. The ratios $\bar a_u$ inserted into the figure are used in Eqs. (9–15) to estimate the upper-surface contributions. Equations (6–8) are used for the lower-surface contributions.

The normal-force coefficient $C_N(\alpha)$ for two slender delta wings, $\Lambda_{LE} = 77.9$ and 70.3 deg, respectively, with $\theta = 6$ deg, determined from Eq. (20), is compared with the experimental results presented by Lampert[4] at several supersonic Mach numbers in Figs. 9 and 10.

The pressure distributions at the trailing edge of a $\Delta_{LE} = 70$-deg wing at $M = 15$ and $\alpha = 5$, 10, and 15 deg obtained by Murman, Rizzi, and Powell[11] from recent solutions of the Euler equations were integrated graphically in order to determine the upper- and lower-surface normal-force contributions. From the equations presented herein, C_N, C^ℓ_N and

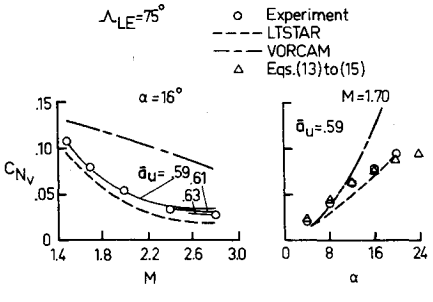

Fig. 6 Representation of experimental $C_{N,v}(M)$ and $C_{N,v}(\alpha)$ from Ref. 9 for a $\Lambda_{LE} = 75$-deg delta wing by curve fitting.

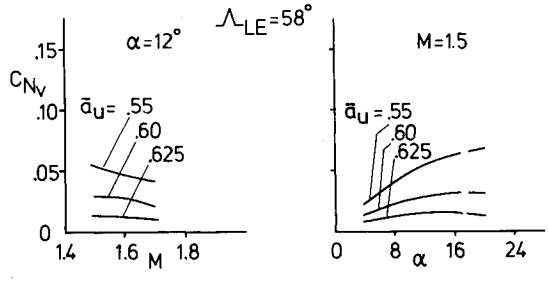

Fig. 7 Sensitivity test of $C_{N,v}(M)$ and $C_{N,v}(\alpha)$ for a $\Lambda_{LE} = 58$-deg delta wing with respect to upper-surface lift-curve slope ratio $\bar a_u$.

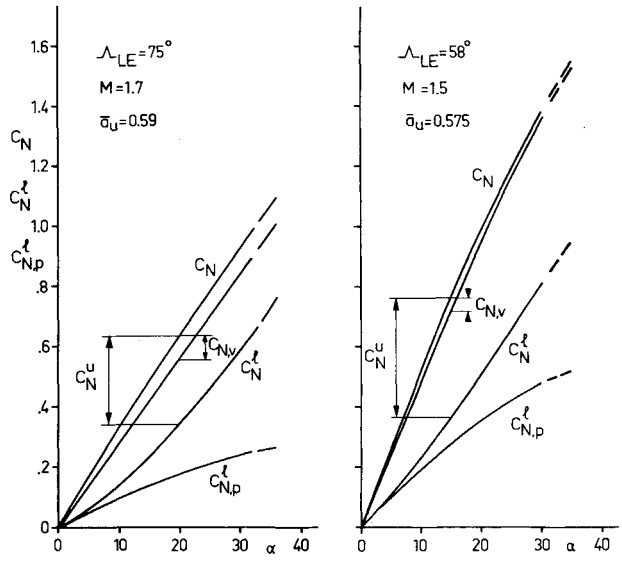

Fig. 8 Subdivision of total normal force of two sharp-edged delta wings in four partial normal-force contributions.

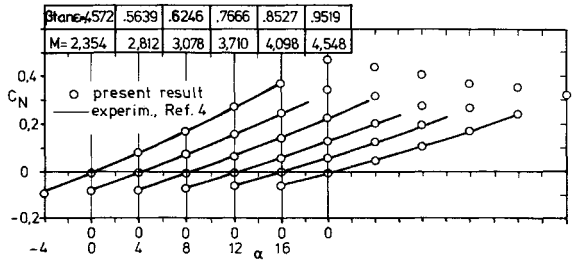

Fig. 9 Representation of the experimental $C_N(\alpha,M)$ for a $\Lambda_{LE}=77.9$-deg delta wing, according to Ref. 4.

C_N^u/C_N vs α were obtained and plotted in Fig. 11 for comparison with the theoretical results.[11]

By the use of Eqs. (6–8) and Eqs. (20) and (19), the total normal-force and the lower-surface normal-force of two delta wings, $\Lambda_{LE}=70.3$ and 58.25 deg, respectively, have been plotted in Figs. 12 and 13 as functions of $\beta\tan\epsilon$ for several angles of attack. Inserted are curves for a constant M_n (the Mach number normal to the leading edge) and also curves labeled $C_N^u=C_N^\ell$ and $C_N^u>\text{const}\times C_N^\ell$, the latter corresponding to the proposed limit curve for the region of interest for the application of leading-edge devices, discussed by Wood and Miller[10] (Figs. 10–12 of Ref. 10).

Discussion

The experimental lift-curve slope for sharp-edged delta wings[3-5] at supersonic speeds in the interval of $0<\beta\tan\epsilon<1.25$ to 1.5 is satisfactorily represented by Eqs. (3–5), as shown in Figs. 2 and 3. The correlation comprises several wing thicknesses, and it is evident from Fig. 3 that the lift-curve slope depends on the thickness. In other words, an increase of thickness decreases the lift-curve slope for $\beta\tan\epsilon>0.5$ (about) and has a weaker but opposite effect for $\beta\tan\epsilon<0.5$. For the present study, in the restricted interval of $0.5<\beta\tan\epsilon<1$, the thickness has been set to $\theta=6$ deg in the chord direction. It is seen from Fig. 2 that the representation of the experimental result[3] is very good for $\theta=6$ deg in the interval of $0<\beta\tan\epsilon<1.25$ for the slender wings, $A=0.858$ and $A=1.433$. Unfortunately, experimental data for $A=3.616$ and $\theta=6$ deg are presented for $\beta\tan\epsilon>0.95$ only, and therefore direct comparisons with the experiment of the present lift-curve slope representation Eqs. (3–5) for this large-aspect ratio wing for $\beta\tan\epsilon<0.95$ cannot be made.

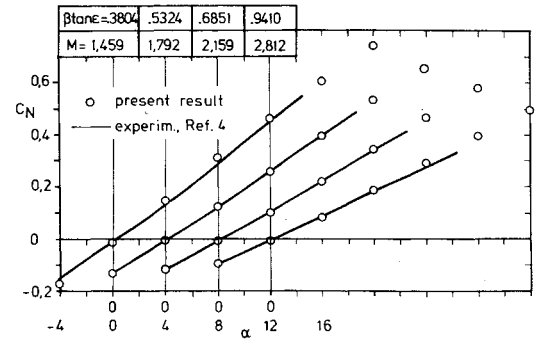

Fig. 10 Representation of the experimental $C_N(\alpha,M)$ for a $\Lambda_{LE}=70.3$-deg delta wing, according to Ref. 4.

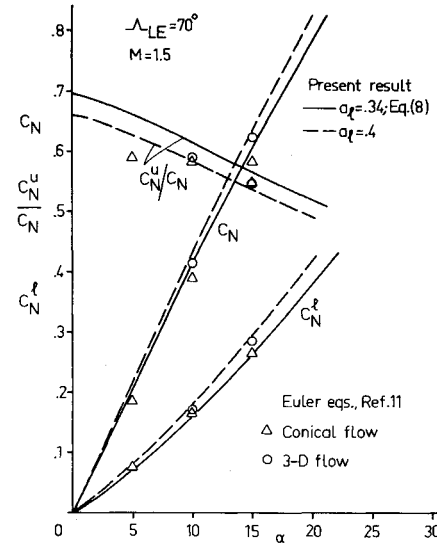

Fig. 11 Comparison between present results on C_N, C_N^ℓ, and C_N^u/C_N vs α and results from two solutions of the Euler equations, Ref. 11.

From Fig. 3, however, it is evident that the lift-curve slopes for the thin ($\theta=2.86$-deg) and thick ($\theta=12.52$-deg) large aspect ratio wings are quite well represented for $\beta\tan\epsilon<1.25$ (approximately). There are good reasons to assume, therefore, that the representation of the $\theta=6$-deg wing is quite good for $\beta\tan\epsilon<0.95$ also. The thin wing is in fact very well represented up to $\beta\tan\epsilon=4$. For increasing thickness and $\beta\tan\epsilon<1.25$, however, a large underprediction of the experimental lift-curve slope appears, telling us that Eq. (4b) exaggerates the influence of the thickness in this supersonic leading-edge flow situation. The use of Eq. (4a) instead of Eq. (4b) for $\beta\tan\epsilon>1.25$ would give a minor improvement of C_{N_β} vs $\beta\tan\epsilon$ for the thicker, large aspect ratio wings in Fig. 3. This indicates that a certain Mach number dependency must be present in the thickness term in Eq. (4a) to obtain a good correlation with the experimental data for $\beta\tan\epsilon>1.25$ for the large aspect wings.

The representation of the lower-surface normal-force contribution,[14] shown in Fig. 4, needs an improvement as to a_ℓ, as discussed in Ref. 14. This would, indeed be worthwhile because a_ℓ is the only unknown in the expression for $C_N^\ell(\alpha)$, according to Eq. (6). The striking simplicity of the C_N^ℓ representation draws benefit from the fluid dynamic crossflow characteristics of disks being independent of the planform.

The upper-surface normal-force coefficient $C_N^u(\bar{\alpha}_n,M)$, presented in Refs. 9 and 10 and plotted in Fig. 5, is very well represented by Eqs. (9–12), although the Mach number correction for the higher Mach numbers could use further improvement. The effectiveness and importance of the angle of attack

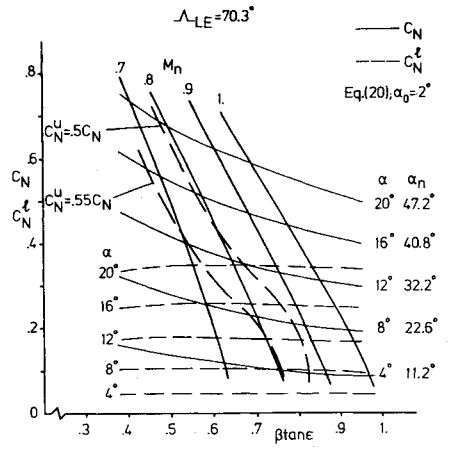

Fig. 12 Chart of C_N^ℓ and C_N vs β tanϵ for a $\Lambda_{LE}=70.3$-deg sharp leading-edge delta wing at several angles of attack.

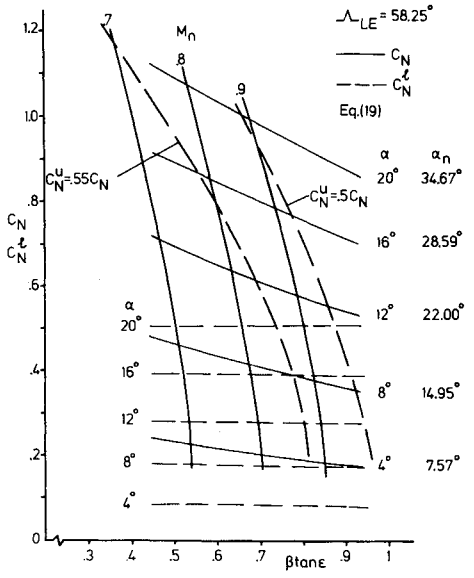

Fig. 13 Chart of C_N^ℓ and C_N vs β tanϵ for a $\Lambda_{LE}=58.25$-deg sharp leading-edge delta wing at several angles of attack.

transformation into $\bar{\alpha}_n$ made in Refs. 9 and 10 should be noticed, because it does emphasize the Mach number dependency and the very small influence of the sweep angle in the upper-surface normal force for large sweep angles. This has made the present representation easier by paving the way for the recognition that the main characteristics of the upper-surface normal force can be captured remarkably well by two fundamental gasdynamic characteristics: the vacuum limit and the real-flow losses (entropy) in combination with the knowledge of the upper-surface lift-curve slope and the relative incidence of the wing.

The curve fit in Fig. 6 by means of Eqs. (13–15) and the experimental result for the $\Lambda_{LE}=75$-deg wing shows that $\bar{a}_u$ in the interval of $0.59<\bar{a}_u<0.63$ provides a good correlation with the experimental date for $1.5<M<2.8$, and, that $\bar{a}_u=0.59$ gives a good correlation vs α at $M=1.7$. The numerical results obtained with the programs LTSTAR and VORCAM are replotted from Ref. 9 and are discussed there. Figure 7 shows the sensitivity of the $C_{N,v}$ of *a* $\Lambda_{LE}=58$-deg wing to some chosen values of $\bar{a}_u$ in the inverval of $0.55<\bar{a}_u<0.625$. The faster decrease of $C_{N,v}$ for an increasing $\bar{a}_u$ compared to the $\Lambda_{LE}=75$-deg wing in Fig. 6 is noticeable.

From the subdivision of the normal-force of the $\Lambda_{LE}=75$- and 58-deg wings (Fig. 8), it is seen that the nonlinear contributions from the upper surface, $C_{N,v}$, and from the lower surface, $C_N^\ell - C_{N,p}^\ell$, are about the same at $\alpha=7$ to 8 deg. For an increasing α, thereafter the faster growth of the nonlinear normal force on the lower surface leads quite soon to a domination of that surface in the production of nonlinear normal-force. The ratio between the upper- and lower-surface normal-force contributions undergoes a large decrease when the angle of attack is increased. Thus, for the smaller, reduced aspect ratio wing (Fig. 8a), C_N^u/C_N^ℓ is equal to 1.41 at $\alpha=10$ deg, 1.0 at 17 deg, and 0.7 at 25 deg. The change is not so fast for the 58-deg wing (Fig. 8b). The sequence is now 1.29 at $\alpha=10$ deg, 1.0 at 18 deg, and 0.83 at 25 deg.

For approximately, $\alpha>25$ deg, the $C_N(\alpha)$ curves in Fig. 8b would already have undergone a more or less dramatic change because of real-flow effects not accounted for herein. Vortex breakdown and the disrupting of the attached (potential flow-like) contribution to the normal-force of the upper surface of the wing will decrease $C_N(\alpha)$ when most of the wing's lift-producing qualities are gradually lost in the stalling process. The flow on the lower surface of the wing is probably more stable and, therefore, the C_N^ℓ and $C_{N,p}^\ell$ curves would have relevance even to high incidences of the wing.

An inspection has shown that Eq. (19) overpredicts Lampert's experimental results[4] up to about 5% for slender delta wings at supersonic speeds. (The comparison is not shown herein.) At present, the source of the discrepancy is not clear. Most probably both upper- and lower-surface normal-force representations contribute to the overprediction. From Figs. 9 and 10 it is seen that zero-angle corrections in Eq. (20) of the order of 1 and 2 deg are sufficient for obtaining very good correlations with the experimental results[4] for the $\Lambda_{LE}=77$-deg wing (Fig. 9) and the $\Lambda_{LE}=70.3$-deg wing (Fig. 10) in the restricted interval of β tanϵ discussed herein. For the latter wing, the comparison comprizes the quite broad interval of $0.38<\beta$ tan$\epsilon<0.95$. It is seen that the correlation for the lowest Mach number β tan$\epsilon<0.5$ is less good, and that for increasing Mach numbers the correlation is very good up till the highest Mach number $M=2.812$. Thereafter, for $\alpha>8$ to 10 deg, a progressive overprediction of C_N begins. The overall excellent correlation at small angles of attack, where the zero-angle corrections in Eq. (20) are negligible, shows that the representation of the linear normal-force contribution to C_N is sufficiently accurate for sweep angles of $\Lambda_{LE}>70$ deg. Whether this is true for smaller sweep angles can only be investigated when relevant experimental results become available. As for the zero-angle corrections, used herein as a kind of sensitivity test, it can be argued that though minor they are still different and thus give an indication of a minor sweep angle dependency of the present analytical representations.

The numerical results[11] from the solutions of the Euler equations for the flow around the $\Lambda_{LE}=70$-deg wing at $M=1.5$, shown in Fig. 11, are obtained both in an assumed conical flow and in three-dimensional flow. In the latter case, the pressure distribution at the trailing edge should not be taken as wholly representative of the normal force of the wing, as is the case for conical flow. From the figure it is seen that the C_N^ℓ and C_N determined in a conical flow are systematically lower than the coefficients determined in a three-dimensional flow.

The representation of C_N^ℓ by Eqs. (6–8) correlates very well with the conical flow results. C_N, however, is overpredicted, which in this case means that C_N^u in conical flow is overpredicted by Eqs. (9–12). The three-dimensional results for C_N^ℓ and C_N, on other hand, are, as a rule, underestimated by the present formulations. It can also be seen that $C_N^u=C_N-C_N^\ell$ is now very well represented by Eqs. (9–12). The overprediction of C_N in a conical flow is in good accord with the observation made in connection with the comparison with experiments,[4] [see comments on Eq. (19)]. The C_N obtained in a three-dimensional flow, therefore, seems overpredicted.

A sensitivity test is made in Fig. 11 by increasing a_ℓ from 0.34 to 0.40 (the broken line curves). The C_N^ℓ and C_N coeffi-

cients are then, at $\alpha = 15$ deg, increased by the same amount, $\Delta C_N^{\ell} = \Delta C_N = 0.0312$. From this it can be estimated that about $a_{\ell} = 0.38$ would give a nearly perfect correlation with the three-dimensional result at $\alpha = 15$ deg and a very small overprediction at $\alpha = 10$ deg. The ratio C_N^u/C_N, formed by the present representations, overpredicts the conical flow result for reasons previously mentioned. Both the theoretical results at $\alpha = 10$ and 15 deg and the result for $a_{\ell} = 0.40$ correlate very well, indicating that the mutual sizes of C_N^u and C_N, though all being different, are practically the same. The large deviation of the conical flow result at $\alpha = 5$ deg most probably is caused by the manual integration of the pressure distribution. The fast decrease of C_N^u/C_N vs α should be observed. More results from the integrations of experimentally and theoretically obtained pressure distributions on delta wings are needed in order to obtain upper- and lower-surface normal forces and to enable a conclusive judgment of the accuracy of both the present result and the solutions of the Euler equations.

From Figs. 12 and 13 it is seen that the nearly constant behavior of the lower-surface normal-force coefficient over $\beta \tan\epsilon$, as noted in Ref. 9, is very well reproduced in the angle-of-attack range inspected. The data points for $\beta \tan\epsilon < 0.5$ in Fig. 12 are probably low, being outside the interval of $\beta \tan\epsilon$ treated herein. The fast decrease of C_N for an increasing Mach number, an early observation from linear supersonic flow theory, is thus almost entirely due to the upper-surface normal-force contribution. As for the curve $C_N^u > \text{const} \times C_N^{\ell}$, it is seen that the enclosed region is lifted to higher angles of attack when the leading-edge sweep angle decreases, and also that the curve for $C_N^u = C_N^{\ell}$ is pushed to a higher M_n. It is the opinion of the present author that leading-edge devices would still be efficient up to at least the latter curve and that designs aiming at keeping the flow attached at the leading edge would be the most rewarding solutions. Arrangements for dropping the leading edge in accord with a parameter function, like $\alpha_n = f\{\alpha(M), \Lambda_{LE}\}$, where the ratios between α and α_n in Figs. 12 and 13 are approximately upheld, would decrease the lift-dependent drag of the full-scale wing by several tons. The angles α_n given in the figures are obtained by geometrical considerations only and do not correspond exactly to real-flow conditions, where interference effects and the nearness of the bow shock will alter the velocity vector from that of the freestream. The correct distribution of drooping along the leading edge, $\delta_{LE}\{\alpha(M), \Lambda_{LE}, x\}$, has to be determined through experiment and/or from solutions of higher-order flow theory.

Conclusions

The first results presented are of a simple engineering method for representing the normal-force characteristics of flat, sharp leading-edge delta wings at supersonic speeds. The method is applicable for Mach numbers above the lower limit for conical flows and below that for supersonic leading-edge flows. The correlation with available experimental results is encouraging. From the results, it is evident that analytic expressions representing the partial normal-force contributions to their substantial parts can be built upon basic aerodynamic and gasdynamic characteristics: the lift-curve slope of the whole wing and of one surface of the wing, the vacuum limit, the pressure loss factor, and the face drag of disks.

Acknowledgment

This work is sponsored by the Material Administration of the Armed Forces, Air Material Department, Missiles Directorate, Sweden, under Contract AU-2154.

References

[1]Stewart, H. J., "The lift of a Delta Wing at Supersonic Speeds," *Quarterly of Applied Mathematics*, Vol. IV:1, Oct. 1946.

[2]Adams, M. C. and Sears, W. R., "Slender-Body Theory—Review and Extension," *Journal of Aeronautical Sciences,* Vol. 2, No. 2, 1953, pp. 85–98.

[3]Lampert, S., "Normal-Force Characteristics of Delta Wings at Supersonic Speeds," *Journal of Aeronautical Sciences*, Vol. 24, Sept. 1957, pp. 667–674.

[4]Lampert, S., "Aerodynamic-Force Chracteristics of Delta Wings at Supersonic Speeds," Jet Propulsion Laboratory, Rept. 20–82, 1954.

[5]Love, E. S., "Investigations at Supersonic Speeds of 22 Triangular Wings Representing Two Airfoil Sections for Each of 11 Apex Angles," NACA Rept. 1238, 1955.

[6]Larson, E. S., "Halvempiriska Uttryck för Lyftkraften hos Deltavinge med Skarp Framkant m h t Profiltjocklek, Anfallsvinkel och Machtal," KTH AERO, Rept. FL 229, Nov. 1961.

[7]Legendre, R., "Ecoulement au Voisinage de la Pointe Avant d'une Aile a Forte Fleche aux Incidences Moyennes," *Recherche Aëronautique*, 1952, 1953.

[8]Edwards, R. H., "Leading-Edge Separation from Delta-Wings," *Journal of Aeronautical Sciences*, Vol. 21, 1954, pp. 134–135.

[9]Wood, R. M. and Miller, D. S., "Assessment of Preliminary Prediction Techniques for Wing Leading-Edge Vortex Flows at Supersonic Speeds," *Journal of Aircraft*, Vol. 22, June 1985, pp. 473–478.

[10]Wood, R. M. and Miller, D. S., "Fundamental Aerodynamic Characteristics of Delta Wings with Leading-Edge Vortex Flows," *Journal of Aircraft*, Vol. 22, June 1985, pp. 479–485.

[11]Murman, E. M., Rizzi, A., and Powell, K. G., "High Resolution Solutions of the Euler Equations for Vortex Flows," *Progress & Supercomputing in Computational Fluid Dynamics*, Birkhäuser-Boston, Inc., 1985.

[12]Hoerner, S. F., *Fluid-Dynamic Drag,* Hoerner Fluid Dynamics, Brick Town, NJ, 1965, pp. 16–13, 16–14, and 16–5.

[13]Larson, E. S., "Crossflow Drag of Finite-Length Rectangular Wing-Bodies," AIAA Paper 85-0451, Jan. 1985.

[14]Larson, E. S., "Lower-Side Normal-Force Characteristics of Delta Wings at Supersonic Speeds," *Journal of Aircraft*, Vol. 23, Sept. 1986, pp. 735–736.